

International Journal of Modern Physics A
© World Scientific Publishing Company

Electroweak couplings and LHC constraints on alternative Z' models in E_6

Richard H. Benavides^a, Luis Muñoz^a, William A. Ponce^b, Oscar Rodríguez^{a,b}, Eduardo Rojas^{c,b}

^a *Facultad de Ciencias Exactas y Aplicadas, Instituto Tecnológico Metropolitano,
Calle 73 No 76 A - 354, Vía el Volador, Medellín, Colombia*

^b *Instituto de Física, Universidad de Antioquia,
Calle 70 No. 52-21, Medellín, Colombia*

^c *Departamento de Física, Universidad de Nariño,
A.A. 1175, San Juan de Pasto, Colombia*

Received Day Month Year

Revised Day Month Year

We report the most general expression for the chiral charges of a Z' gauge boson coming from an E_6 unification model, as a function of the electroweak parameters and the charges of the $U(1)$ factors in the chain of subgroups. These charges are valid for an arbitrary Higgs sector and only depend on the branching rules of the E_6 fundamental representation and the corresponding rules for the fermionic representations of their subgroups. By assuming E_6 unification, the renormalization group equations (RGE) allow us to calculate the electroweak parameters at low energies for most of the chains of subgroups in E_6 . From RGE and unitary conditions, we show that at low energies there must be a mixing between the gauge boson of the standard model hypercharge and the Z' . From this, it is possible to delimit the preferred region in the parameter space for a breaking pattern in E_6 . In general, without unification, it is not viable to determine this region; however, for some models and under certain assumptions, it is possible to limit the corresponding parameter space. By using the most recent upper limits on the cross-section of extra gauge vector bosons Z' decaying into dileptons from the ATLAS data at 13 TeV with accumulated luminosities of 36.1 fb^{-1} and 13.3 fb^{-1} , we report the 95% C.L. lower limits on the Z' mass for the typical E_6 benchmark models. We also show the contours in the 95% C.L. of the Z' mass bounds for the entire parameter space of E_6 .

Keywords: Keyword1; keyword2; keyword3.

PACS numbers:

1. Introduction

From a group theory point of view, there are several ways to break the E_6 symmetry down to the standard model (SM) one. Although some of the breaking patterns have been explored in the literature so far, a systematic study of the phenomenology for all the alternative ways has not been done as far as we know. In general,

2 *Richard H. Benavides, Luis Muñoz, William A. Ponce, Oscar Rodríguez, Eduardo Rojas*

intricate models are not appealing. A way to look for new models with a moderate fermion content is to consider alternative versions of the models already known in the literature.^{1–10} Our work represents a first step in this direction. One of the first alternative models was “flipped $SU(5)$ ”,^{1,11} which produces a symmetry breaking for $SO(10)$ down to $SU(5) \otimes U(1)$, where the $U(1)$ factor contributes to the electric charge, and as such, its basic predictions for $\sin^2 \theta_W$ and the proton decay are known to be different from those of $SU(5)$.¹ An alternative model for the flipped $SU(5)$ is $SO(10) \otimes U(1)_N$, where the right-handed neutrino has zero charge under the $U(1)_N$ group allowing a Majorana mass term.^{5,12} The alternative versions of the left-right model are also well known in the literature,^{4,13} as in the latter case, one of these models allows for a right-handed neutrino component effectively inert.⁴

The alternative models have been useful in the study of the grand unified theories (GUTs) phenomenology, for example, for the E_6 subgroup $SU(2)_R \otimes SU(6)$ and some of its three alternative versions, the gauge mediated proton decay operators are suppressed at leading order due to the special placement of matter fields in the unified multiplets.^{9,14–18}

Heavy neutral gauge bosons are a generic prediction of many types of new physics beyond the SM. In addition, these extra $U(1)'$ symmetries serve as an important model-building tool¹⁹ (for example, to suppress strongly constrained processes) giving rise, after spontaneous $U(1)'$ symmetry breaking, to physical Z' vector bosons. Thus, with the upgrade of the luminosity and the energy of the LHC, there exists a real possibility for the on-shell production of a Z' boson.^{20,21}

All representations of the E_6 gauge group^{22,23} are anomaly-free and the fundamental **27**-dimensional representation is chiral and can accommodate a full SM fermion generation. As a consequence, E_6 -motivated Z' bosons arise naturally in many popular extensions of the SM,^{2,20,24,25} both in top-down and bottom-up constructions. Some of the E_6 subgroups, such as the original unification groups $SU(5)$ and $SO(10)$, and the gauge group of the left-right symmetric models $SU(4)_C \otimes SU(2)_L \otimes SU(2)_R$, play central roles in some of the best motivated extensions of the SM. Furthermore, the complete E_6 -motivated Z' family of models appears in a supersymmetric bottom-up approach exploiting a set of widely accepted theoretical and phenomenological requirements.²⁶ The one-parameter Z' families in reference,²⁷ denoted as $\mathbf{10} + x\bar{\mathbf{5}}$, $d - xu$ and $q + xu$, where $\mathbf{10}$ and $\bar{\mathbf{5}}$ are $SU(5)$ representations, can also be discussed within the E_6 framework.²⁸

For all these reasons there is an expectation that an E_6 Yang-Mills theory, or a subgroup of E_6 containing the SM in a non-trivial way, might be part of a realistic theory.²⁹ If a heavy vector boson is seen at the LHC or at an even more energetic collider in the future, aspects of the E_6 symmetry group will be central to the discussion of what this resonance might be telling us about the fundamental principles of nature.

The discrimination between Z' models could be challenging at the LHC due to the small number of high resolution channels at hadron colliders. Another reason why the determination of the underlying symmetry structure is not straightforward

is that the mass eigenstate of the Z' is, in general, a linear combination of some of the underlying Z' charges with the ordinary Z boson of the SM. Hence, it is useful to reduce the theoretical possibilities or at least to have a manageable setup. This work represents an attempt in this direction and serves to spotlight a few tens of models in the two-dimensional space of E_6 -motivated Z' models.

All the E_6 breaking patterns and branching rules have been tabulated in Ref.²⁹ In references^{2,7} all the chains of subgroups were tabulated. The aim of the present work is to set the impact of the latest LHC constraints on the possible embeddings of the SM in the subgroups of E_6 .

It is important to remark that many interesting phenomenological models appear in a natural way in E_6 breaking patterns, such as the proton-phobic, Z_{η} , neutron-phobic, $Z_{\eta'}$, (vector bosons which at zero momentum transfer do not couple to protons and neutrons, respectively), leptophobic Z_{ℓ} (with zero couplings to leptons) and vector bosons from supersymmetric models, as for example the Z_N model,^{5,12} *etc.* We will show a more complete list later.

The study reported here is a continuation of the analysis started in Ref.⁷ where the quantum numbers of the abelian gauge groups in alternative chains of subgroups of E_6 were calculated. Several of the subgroups shown there are well known in the literature; however, as far as we know, the phenomenology of many of these models have not been studied. Of particular importance for the electroweak constraints are the Z' chiral charges of the SM fermions which depend on the chosen chain of subgroups. In the present work, we show the general expression for these charges and determine the preferred region in the parameter space for some breaking patterns. We also establish that the mixing between the Z' charges and the SM hypercharge is a measure of the deviation of the parameter space at low energies respect to their unification values. We demonstrate that the presence of this mixing stems from the gauge coupling splitting at low energies.

The paper is organized as follows: In Section 2 we derive general expressions for the electroweak (EW) charges of a Z' in E_6 as a function of the mixing angles and the charges of an arbitrary $U(1)$ in E_6 . In section 3 we show that even for a group with orthonormal charges at low energies there is a kinetic mixing due to the splitting of the gauge coupling constants. In section 4 we revise the existing literature about models based on E_6 subgroups and their embeddings. By assuming E_6 unification the renormalization group equations (RGE) allow us to determine the parameter space of the Z' associated with some of these models. For this purpose, we take the expressions for the mass scales and couplings of the Robinett and Rosner (RR) work.² In this section, we also point out the existence of non-trivial models which, to the best of our knowledge, have not been studied in the literature. In section 5 we delimit the parameter space when we put aside the unification hypothesis as it usually happens for effective models at low energies. In section 6 the 95% C.L. exclusion limits on the neutral boson masses for the entire E_6 -motivated Z' parameter space are shown.

4 *Richard H. Benavides, Luis Muñoz, William A. Ponce, Oscar Rodríguez, Eduardo Rojas*

2. General expressions

Owing to the fact that the rank of E_6 is 6, for chains of subgroups with regular embeddings (those preserving the rank) the most general form of the group associated with the low-energy effective model is^{2,29} $SU(3)_C \otimes SU(2)_L \otimes \prod_\kappa U(1)_\kappa$, with $\kappa = a, b, c$; where the $U(1)$ factors come from the chains of subgroups of E_6 . In order to reproduce the $SU(3)_C \otimes SU(2)_L \otimes U(1)_Y$ symmetry of the SM it is necessary that the SM hypercharge Y be a linear combination of the $U(1)_\kappa$ charges Q_κ . If g is the $SU(2)_L$ coupling constant and A_{3L}^μ the gauge boson associated with the third component of the weak isospin, then the neutral current Lagrangian \mathcal{L}_{NC} for the most general case is

$$-\mathcal{L}_{NC} = gJ_{3L}^\mu A_{3L\mu} + g_a J_a^\mu A_{a\mu} + g_b J_b^\mu A_{b\mu} + g_c J_c^\mu A_{c\mu} , \quad (1)$$

where g_κ and A_κ^μ represent the gauge coupling constant and the gauge field associated with the $U_\kappa(1)$ symmetry, respectively. The fermion currents J_κ^μ are given by

$$J_\kappa^\mu = \sum_f \bar{f} \gamma^\mu [\epsilon_L^\kappa(f) P_L + \epsilon_R^\kappa(f) P_R] f, \quad (2)$$

where f runs over all fermions in the **27** representation of E_6 , which is the fundamental representation. The chirality projectors are defined as usual i.e., $P_{L,R} = (1 \pm \gamma^5)/2$ and $f_{L,R} = P_{L,R} f$. The chiral charges are $\epsilon_L(f) = Q_k(f_L)$ and $\epsilon_R(f) = -Q_k(f_L^c)$. The $U(1)_\kappa$ charges satisfy the E_6 normalization condition $\sum_{f \in \mathbf{27}} Q_\kappa^2(f) = 3$ (see Table 3 in appendix Appendix D). As a consequence of this, the electric charge operator Q_{em} is given by

$$Q_{em} = T_3 + Y = T_3 + \sqrt{\frac{5}{3}} Q_Y^{E_6} ,$$

where T_3 is the third component of weak isospin and $Q_Y^{E_6}$ is the E_6 normalized SM hypercharge.

By means of an orthogonal transformation \mathcal{O} we can pass from the gauge interaction basis to the basis in which one of the fields can be identified with the SM hypercharge B^μ associated with the $U(1)_Y$ symmetry. If we define such a rotation through ^a

$$\begin{pmatrix} A_{3L}^\mu \\ A_a^\mu \\ A_b^\mu \\ A_c^\mu \end{pmatrix} = \mathcal{O} \begin{pmatrix} A_{3L}^\mu \\ B^\mu \\ Z'^\mu \\ Z''^\mu \end{pmatrix} = \begin{pmatrix} 1 & 0 & 0 & 0 \\ 0 & O_{11} & O_{12} & O_{13} \\ 0 & O_{21} & O_{22} & O_{23} \\ 0 & O_{31} & O_{32} & O_{33} \end{pmatrix} \begin{pmatrix} A_{3L}^\mu \\ B^\mu \\ Z'^\mu \\ Z''^\mu \end{pmatrix} , \quad (3)$$

^a The absence of mixing between A_{3L}^μ and the other fields is related to the strong constraints on the Z and Z' mixing angle by low energy experiments,³⁰ consequently, the only mixing between the hypercharge and A_{3L}^μ is parametrized by the Weinberg angle θ_W .

then the Lagrangian (1) can be written as

$$-\mathcal{L}_{NC} = gJ_{3L}^\mu A_{3L\mu} + g_Y J_Y^\mu B_\mu + g_{Z'} J_{Z'}^\mu Z'_\mu + g_{Z''} J_{Z''}^\mu Z''_\mu . \quad (4)$$

In order to keep invariant the Lagrangian, the currents must transform with the same orthogonal matrix

$$g_Y J_Y^\mu = g_a J_a^\mu O_{11} + g_b J_b^\mu O_{21} + g_c J_c^\mu O_{31} , \quad (5)$$

$$g_{Z'} J_{Z'}^\mu = g_a J_a^\mu O_{12} + g_b J_b^\mu O_{22} + g_c J_c^\mu O_{32} , \quad (6)$$

$$g_{Z''} J_{Z''}^\mu = g_a J_a^\mu O_{13} + g_b J_b^\mu O_{23} + g_c J_c^\mu O_{33} . \quad (7)$$

The exact expression for the orthogonal matrix is given in appendix Appendix A. In order to obtain the SM as an effective theory at low energies, the breaking $U_a(1) \otimes U_b(1) \otimes U_c(1) \longrightarrow U(1)_Y$ must take place. If so, it is possible to find three real coefficients k_a , k_b and k_c such that

$$Y = \sqrt{\frac{5}{3}} Q_Y^{E_6} = k_a Q_a + k_b Q_b + k_c Q_c . \quad (8)$$

From Eqs. (2) and (8) we obtain for the currents the relation

$$J_Y^\mu = k_a J_a^\mu + k_b J_b^\mu + k_c J_c^\mu . \quad (9)$$

In Tables 4 to 7 (in appendix Appendix D) we have reported the values of k_κ for the models considered in this work. By comparing Eq. (9) with Eq. (5), we get the following expressions:

$$g_a O_{11} = k_a g_Y , \quad g_b O_{21} = k_b g_Y , \quad g_c O_{31} = k_c g_Y , \quad (10)$$

which, along with the orthogonal condition $O_{11}^2 + O_{21}^2 + O_{31}^2 = 1$, impose a constraint on the g_a , g_b and g_c coupling constants, namely:

$$\left(\frac{k_a}{g_a}\right)^2 + \left(\frac{k_b}{g_b}\right)^2 + \left(\frac{k_c}{g_c}\right)^2 = \left(\frac{1}{g_Y}\right)^2 . \quad (11)$$

From these expressions and the explicit form of the rotation matrix \mathcal{O} (see Appendix A) we get the Z' chiral charges (see Appendix B)

$$g_{Z'} \epsilon_{L,R}^{Z'} = A_{L,R} \cos \theta + B_{L,R} \sin \theta , \quad (12)$$

$$g_{Z''} \epsilon_{L,R}^{Z''} = -A_{L,R} \sin \theta + B_{L,R} \cos \theta , \quad (13)$$

where

$$A_{L,R} = \frac{g_c}{\hat{\alpha}_c} \left(\frac{k_a \epsilon_{L,R}^b}{\hat{\beta}} - \hat{\beta} k_b \epsilon_{L,R}^a \right) , \quad (14)$$

$$B_{L,R} = g_Y \left(-\frac{k_a \epsilon_{L,R}^a + k_b \epsilon_{L,R}^b}{\hat{\alpha}_c} k_c + \hat{\alpha}_c \epsilon_{L,R}^c \right) , \quad (15)$$

6 *Richard H. Benavides, Luis Muñoz, William A. Ponce, Oscar Rodríguez, Eduardo Rojas*

and θ is an angle of the rotation matrix \mathcal{O} which can take any value between $-\pi$ and π . Here $\hat{\alpha}_c = g_c \sqrt{\frac{k_a^2}{g_a^2} + \frac{k_b^2}{g_b^2}} = \sqrt{\frac{g^2}{g^2} \cot^2 \theta_W - k_c^2}$, and $\hat{\beta} = \frac{g_a}{g_b}$. In order to have the chiral charges properly normalized in E_6 we define

$$g_{Z'} \equiv \frac{1}{\hat{\alpha}_c \hat{\beta}} \left(\cos^2 \theta g_c^2 (k_a^2 + \hat{\beta}^4 k_b^2) - 2\hat{\beta}(1 - \hat{\beta}^2) g_c g_Y k_a k_b k_c \cos \theta \sin \theta \right) \quad (16)$$

$$+ \hat{\beta}^2 g_Y^2 ((k_a^2 + k_b^2) k_c^2 + \hat{\alpha}_c^4 \sin^2 \theta)^{1/2}, \quad (17)$$

which reduces to the Georgi-Glashow well known result $\sqrt{\frac{5}{3}} g_Y = \sqrt{\frac{5}{3}} g \tan \theta_W$ for $g_c = g_a = g_b$. These charges reproduce the electroweak charges of trinification and the left-right symmetric model which are well known in the literature (for additional references look into our previous work¹³). Since $g_{Z'} \epsilon_{L,R}^{Z'}(\theta + \pi/2) = g_{Z''} \epsilon_{L,R}^{Z''}(\theta)$, the parameter space associated with the Z'' boson is the same as that of the Z' boson.

3. Kinetic mixing from gauge coupling splitting

Because all the generators Q_{ij}^a associated with the neutral currents can be diagonalized simultaneously the corresponding fields can be written as $A^\mu = A^{\mu a} T_{ij}^a = A^{\mu a} Q^a(i) \delta_{ij}$, where $Q^a(i)$ stands for the charge of the i -fermion in the fundamental representation. For these fields the most general lagrangian is given by

$$\begin{aligned} \text{Tr}[F_{\mu\nu} F^{\mu\nu}] &= \text{Tr}[F_{\mu\nu}^a T^a F^{\mu\nu b} T^b] \\ F_{\mu\nu}^a F^{\mu\nu b} \sum_{i,j} Q^a(i) \delta_{ij} Q^b(j) \delta_{ji} &= F_{\mu\nu}^a F^{\mu\nu b} \sum_i Q^a(i) Q^b(i). \end{aligned} \quad (18)$$

When i runs over the fermions in a multiplet of a simple group (or a semisimple group that comes from the breaking of a simple Lie group) the charges are orthonormal

$$\sum_i Q^a(i) Q^b(i) = \sum_i \epsilon^a(i) \epsilon^b(i) = \delta_{ab}. \quad (19)$$

It is not possible to generate a kinetic mixing term to tree level because $F^{\mu\nu a}$ transforms with an orthogonal matrix; however, at low energies it is possible to generate a kinetic mixing by one-loop corrections.^{20, 31–33} As we will show, a source of kinetic mixing at low energies is the splitting of the values of the coupling strengths. By unitarity the currents should transform in the same way as the fields; if we transform from the group basis to a basis where one of the fields corresponds to the vector field associated with the SM hypercharge B_μ , the corresponding expression for the currents is

$$\begin{pmatrix} g J_{3L}^\mu \\ g_Y J_Y^\mu \\ g_{Z'} J'^\mu \\ g_{Z''} J''^\mu \end{pmatrix} = \mathcal{O}^T \begin{pmatrix} g J_{3L}^\mu \\ g_a J_a^\mu \\ g_b J_b^\mu \\ g_c J_c^\mu \end{pmatrix} = \begin{pmatrix} 1 & 0 & 0 & 0 \\ 0 & O_{11} & O_{12} & O_{13} \\ 0 & O_{21} & O_{22} & O_{23} \\ 0 & O_{31} & O_{32} & O_{33} \end{pmatrix}^T \begin{pmatrix} g J_{3L}^\mu \\ g_a J_a^\mu \\ g_b J_b^\mu \\ g_c J_c^\mu \end{pmatrix}. \quad (20)$$

From the definitions $g_Y J_Y^\mu(f) = \sum_\kappa \mathcal{O}_{1\kappa} g_\kappa J_\kappa^\mu(f)$, $g_{Z'} J_{Z'}^\mu = \sum_\lambda \mathcal{O}_{2\lambda} g_\lambda J_\lambda(f)^\mu$, and the Eq. 2 we obtain the expressions

$$g_Y Y = \sum_\kappa \mathcal{O}_{1\kappa} g_\kappa \epsilon^\kappa(f), \quad (21)$$

$$g_{Z'} \epsilon_{Z'} = \sum_\lambda \mathcal{O}_{2\lambda} g_\lambda \epsilon^\lambda(f). \quad (22)$$

By taking the dot product of the SM hypercharge g_Y and the Z' charges $g_{Z'} \epsilon_{Z'}$ we obtain

$$\begin{aligned} g_Y \mathbf{Y} \cdot g_{Z'} \epsilon_{Z'} &\equiv \sum_{f \in 27} g_Y Y(f) g_{Z'} \epsilon_{Z'}(f) \\ &= \sum_{\kappa, \lambda} \sum_{f \in 27} \mathcal{O}_{1\kappa} g_\kappa \epsilon^\kappa(f) \mathcal{O}_{2\lambda} g_\lambda \epsilon^\lambda(f) \end{aligned} \quad (23)$$

$$= 3 \sum_\kappa \mathcal{O}_{1\kappa} \mathcal{O}_{\kappa 2}^T g_\kappa^2, \quad (24)$$

where \mathcal{O} is the rotation matrix (3). Here we made use of the E_6 orthonormality relation $\sum_{f \in 27} \epsilon^\kappa(f) \epsilon^\lambda(f) = 3\delta_{\kappa\lambda}$ between the $U(1)_\kappa$ charges that come from a chain of subgroups. By assuming that the three couplings are identical $g_a = g_b = g_c$ we obtain $g_Y \mathbf{Y} \cdot g_{Z'} \epsilon_{Z'} = 3g_a^2 \sum_\kappa \mathcal{O}_{1\kappa} \mathcal{O}_{\kappa 2}^T = 3g_a^2 \delta_{12} = 0$, otherwise

$$\mathbf{Y} \cdot \epsilon_{Z'} = \sum_{f \in 27} Y(f) \epsilon_{Z'}(f) \neq 0. \quad (25)$$



Fig. 1. Z'_μ - B_μ kinetic mixing.

This result shows that the orthonormality of the SM hypercharge and the Z' charges is only guaranteed when all the three couplings are equal as it happens in unification; for the remaining cases a kinetic mixing is generated by the one-loop diagram in figure 1 (even for complete fermion representations).

In general, at low energies the gauge couplings g_κ are different each other due to the RGE; thus, as will be shown below, the Z' charges associated with a chain of subgroups in E_6 are no longer orthonormal to the SM hypercharge. It is important to notice that the 2-loop corrections are important for the RGE since they modify in a considerable way the mass unification scales; however, for several models, unification does not impose relations between the SM electroweak couplings in such a way that the consistency of the model does not depend on high order corrections and the SM values for the $\alpha_i = g_i^2/(4\pi)$ can be considered as input parameters. Under these conditions, the 1-loop coupling strengths² g_κ associated to the extra $U(1)$ abelian symmetries differs in just a few percent respect to the 2-loop result at the

8 *Richard H. Benavides, Luis Muñoz, William A. Ponce, Oscar Rodríguez, Eduardo Rojas*

electroweak scale, since the boundary condition on the SM parameters is imposed at the same energy scale.³⁴

The phenomenological consequences of the $B_\mu - Z'_\mu$ kinetic mixing is a modification of the Z charges.^{20,32,33} In turn, this contribution represents a non-zero value for the Z - Z' mixing angle, which is strongly constrained by Z -pole observables and low energy constraints.³⁰

It is important to notice that something similar happens in the standard model where the chiral charges of the photon $Q = T_3 + Y$ and are not orthogonal to those of the Z boson $T_3 - \sin^2 \theta_W Q$, hence, one effective kinetic mixing arise by one-loop corrections.³⁵

4. Benchmark models in E_6

The maximal subgroups of E_6 which can include $SU(3) \otimes U(1)$ as an unbroken symmetry are²⁹ Sp_8 , $SU(2) \otimes SU(6)$, $SO(10) \otimes U(1)$, F_4 , and $[SU(3)]^3$. By imposing the SM gauge group as an intermediate step in the breaking chain $E_6 \rightarrow SM \rightarrow SU(3) \otimes U(1)_{\text{EM}}$, the subgroups Sp_8 and F_4 can be eliminated. So, from now on we are going to focus only on the breaking chains in figure (2) which, by the way, sets part of our convention in the sense that we refer to A as the chain belonging to $SO(10) \otimes U(1)$, B to the chain $SU(2) \otimes SU(6)$, \dots , etc.

4.1. $SO(10) \otimes U(1)$

In what follows, the models will also be denoted according to the generalized RR notation.⁷ The list of models and their respective RR notations are shown in table 1.

In E_6 there are only three chains of subgroups for which the SM hypercharge $U(1)_Y$ (U_{32I} in RR notation) appears in a natural way. Two of them, $A1_{RI}$ and $A1_{AI}$ (see figure (3) and table 4), go through $SO(10) \otimes U(1)$ and that is one of the reasons why this group have been widely studied in GUTs. The $A1_{RI}$ chain of subgroups corresponds to the embedding of the Georgi-Glashow unification model³⁶ $SU(5)$ in E_6 through the breaking²⁹ $E_6 \rightarrow SO(10) \otimes U(1)_{42R} \rightarrow SU(5) \otimes U(1)_{\chi RI} \otimes U(1)_{42R} \rightarrow SU(3) \otimes SU(2) \otimes U(1)_{32I} \otimes U(1)_{\chi RI} \otimes U(1)_{42R}$. The charges of $U(1)_{\chi RI}$ and $U(1)_{42R}$ corresponds to those of¹ Z_χ and Z_ψ (see table 3), respectively; these models are well known in E_6 (see table 1). After we rotate to the mass eigenstate basis two vector bosons Z' and Z'' appear in addition to the SM fields. When the mixing between the SM Z and the extra neutral vector bosons is zero^{30,37-39} the Z' and Z'' fields are a linear combination of²⁴ Z_χ and Z_ψ

$$Z' = \cos \beta Z_\chi + \sin \beta Z_\psi. \quad (26)$$

By varying β from 0 to $\pi/2$ the parameter space in figure (6) corresponds to the vertical line which goes through Z_ψ ($U(1)_{42R}$) and Z_χ ($U(1)_{\chi RI}$). That is the parameter space of the models orthogonal to the SM hypercharge, i.e., $\sum_{f \in 27} Q_{Z'}(f)Y(f) = 0$, where $Q_{Z'}(f)$ is the Z' charge of the fermion f and $Y(f)$ the SM hypercharge. As was shown in section 3, this vertical line also corresponds

Table 1. E_6 -motivated Z' benchmark models and their generalized RR notations.⁷ The Z_I , $Z_{\mathcal{J}}$, and $Z_{\mathcal{L}}$ bosons are blind, respectively, to up-type quarks, down-type quarks, and SM leptons. Similarly, the $Z_{\mathcal{U}}$ and the $Z_{\mathcal{V}}$ are gauge bosons which do not couple (at vanishing momentum transfer and at the tree level) to neutrons and protons, respectively. The Z_{B-L} couples purely vector-like while the Z_{ψ} has only axial-vector couplings to the ordinary fermions. For convenience the models with the same multiplet structure as the Z_{χ} are referred to as $U_{\chi XY}$. The Z_S model does not have RR notation

Z'	Z_R^2	Z_d^{28}	$-Z_I^2$	$-Z_{L_1}^2$	$-Z_{R_1}^2$	$Z_{\mathcal{V}}^{28}$
RR	U_R	U_A	U_I	U_{33}	$U_{21\bar{R}}$	$U_{21\bar{A}}$
Z'	$-Z_{\mathcal{U}}^{28,40}$	$-Z_{B-L}^{41}$	Z_{ALR}^4	$-Z_{\mathcal{L}}^{32}$	Z_{ψ}^2	Z_{χ}^2
RR	$U_{21\bar{I}}$	U_{31R}	U_{31A}	U_{31I}	U_{42R}	$U_{\chi RI}$
Z'	$Z_N^{5,12}$	$Z_{\chi^*}[\text{flipped-}SU(5)]^1$	Z_{η}^3	$Z_Y^{42,43}$	$Z_S^{44,45}$	$Z_{331G}^{13,40,46}$
RR	$U_{\chi AI}$	$U_{\chi RA}$	U_{51I}	U_{32I}		$U_{21\bar{I}}, U_{33}$

to the parameter space for any E_6 -motivated Z' at the unification limit; however, owing to the RGE, at low energies the values of the g_{κ} couplings will depend on the specific details of the breaking pattern. Because at low energies the couplings are no longer identical, the Z' parameter space acquires a component in the SM hypercharge axis in figure (6), which is equivalent to a kinetic mixing of the form²⁸

$$Z' = \cos \alpha \cos \beta Z_{\chi} + \sin \alpha \cos \beta Y + \sin \beta Z_{\psi} . \quad (27)$$

Due to this mixing the Z' parameter space will be out of the unification vertical line as is shown for some models in figure (6).

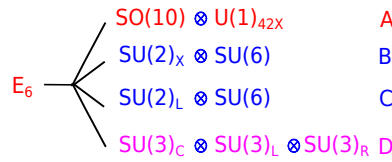


Fig. 2. E_6 maximal subgroups

The other chain of subgroups in which the SM hypercharge appears naturally is $A1_{AI}$. The $SU(5)$ is the Georgi-Glashow one, but the factor $U(1)_{\chi AI}$ is an alternative version of U_{χ} ($U(1)_{\chi RI}$), which is known in the literature as U_N . Figure 3 shows the embedding of $SU(5) \otimes U(1)_N$ (i.e., $SU(5) \otimes U(1)_{\chi AI}$) in E_6 . This is the symmetry group of the Exceptional Supersymmetric Standard Model (ESSM),¹² which is obtained from the E_6 charges by requiring vanishing $U(1)_N$ charges for right-handed neutrinos.

Table 4 shows the six possible ways to embed $SU(5)$ into $SO(10) \otimes U(1) \subset E_6$ (all the chains of subgroups of the form $A1_{XY}$ can be seen in figure (3)); from these, the $A1_{RA}$ chain corresponds to the flipped $SU(5)$.¹

10 *Richard H. Benavides, Luis Muñoz, William A. Ponce, Oscar Rodríguez, Eduardo Rojas*

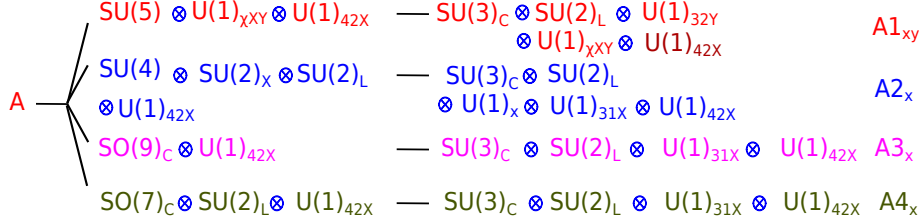


Fig. 3. $E_6 \rightarrow SO(10) \otimes U(1)_{42X}$ chains of subgroups, where $X, Y = R, I, A$ and $X \neq Y$.

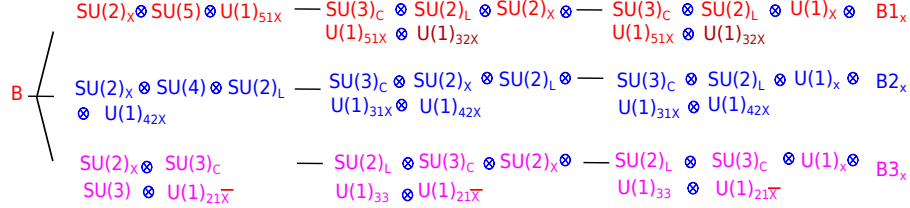
Taking as inputs the values of the fine-structure constant and the corresponding quantities for the strong and weak interactions, we find the strength couplings at low energies by using the one-loop RGE equations;² however, we always find that for the $A1_{XY}$ chains of subgroups it is not possible to get the right order between the unification scales. That problem is related to the wrong prediction of the Weinberg angle in $SU(5)$. Although it is not possible to have a consistent picture for the embeddings $SU(5) \otimes U(1) \subset SO(10) \otimes U(1) \subset E_6$, there are solutions in most of the remaining E_6 breaking patterns.

4.1.1. $SU(4) \otimes SU(2)_L \otimes SU(2) \otimes U(1) \subset SO(10) \otimes U(1) \subset E_6$

From the three chains of subgroups $A2_X$ in figure (3) we can get low-energy E_6 models (LEE6Ms) *i.e.*, models where at least one of the neutral currents in Eq. (9) does not contribute to the hypercharge, therefore, the corresponding vector boson is not necessary to have a consistent model. Usually, the fermion content of these models is smaller than the fundamental representation of E_6 .

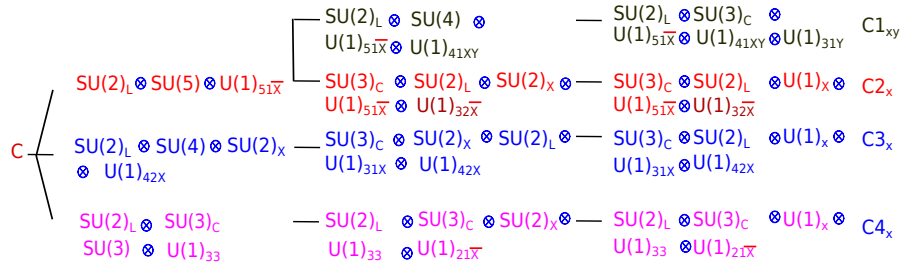
The $A2_R/U(1)_{42R}$ chain^b is the Pati-Salam model^{41,47} (see figure (3)). The EW charges of this model are the same as those of $B2_R/U_{42R}$ (see figure (4)) and $C3_R/U_{42R}$ (see figure (5)) and are the same as the Left-Right (LR) symmetric model. The $A2_A/U_{42A}$ chain of subgroups corresponds to the alternative left-right model Z_{ALR} .⁴ The EW charges for this model were reported in¹³ and are identical to those of $B2_A/U_{42A}$ and $C3_A/U_{42A}$. $A2_I$ is a new model in the literature even though is closely related to the second alternative model obtained from trinification;¹³ the difference lies in the Abelian factor U_{42I} (in¹³ Y is a linear combination of U_{31I} and $U(1)_I$, while in the $SO(10)$ embedding U_{42I} is in place of U_I). Identical EW charges are obtained from $B2_I$ and $C3_I$. Note that the coefficients of the hypercharge in $A3_I$ and $A4_I$ are identical to those of $A2_I$; however, due to the absence of the $U(1)_I$ factor in the chain of subgroups, in Eq. (12) there is no mixing with the corresponding vector boson Z_I . In E_6 the parameter space for every Z' of the $A2_X$ chain coincides with those of $C3_X$ in figure 6.

^b $A2_R/U(1)_{42R}$ denote the chain of subgroups $A2_R$ without the $U(1)_{42R}$ factor.

Fig. 4. $E_6 \rightarrow SU(2)_X \otimes SU(6)$ chains of subgroups, where $X = R, I, A$.

4.2. $SU(2) \otimes SU(6) \subset E_6$

The third chain of subgroups in which the SM hypercharge $U(1)_Y$ appears in a natural way is the $B1_I$ in figure (4). This model occurs in Calabi-Yau compactifications in string theory³ and is commonly denoted as Z_η . The charges of this model correspond to those of $U(1)_{51I}$ (see Table 3). In this chain of subgroups the $SU(5)$ is the same as that of Georgi-Glashow; however, the $U(1)_{51}$ factor is different from the corresponding factor in the embedding through $SO(10)$. The other two chains in $SU(2)_X \otimes SU(6)$ are $B2_X$ and $B3_X$. For these chains, the Z' charges of the LEE6Ms correspond to those of the Pati-Salam and trinification models, and their corresponding alternative versions, which have been studied in the previous section and in reference.¹³ New models appear in the chains of subgroups containing $SU(2)_L \otimes SU(6)$; of particular interest are $C2_X$, which contain a $SU(5)$ different from the Georgi-Glashow one. This new $SU(5)$ allows a solution for the mass scales in E_6 from the one-loop RGE² (we saw above that such a solution is not possible either in the Georgi-Glashow model or its alternative versions). The same is true for the $C1_{xy}$ chains of subgroups. The chains $C3_X/U(1)_{42X}$ and $C4_X$ have the same Z' charges as the Pati-Salam and trinification models, respectively. The low-energy Z' charges for $C1_X$, $C2_X$ and $C3_X$ as a function of the θ mixing angle (see Eq. (12)) are shown in the Sanson-Flamsteed projection in figure (6).

Fig. 5. $E_6 \rightarrow SU(2)_L \otimes SU(6)$ chains of subgroups, where $X, Y = R, I, A$ and $X \neq Y$.

4.3. $SU(3) \otimes SU(3) \otimes SU(3)$

The $SU(3) \otimes SU(3) \otimes SU(3)$ is the gauge group of trinification.^{23, 48–51} In table 7 are shown the three possible chains of breakings for this group. As was shown in reference,¹³ the charges of the three chains reduce to those of the universal 331 vector boson Z_{331G} (see table 2 for the LHC constraints). A detailed study of these models and their EW constraints was presented in reference.¹³

5. Low-energy models without unification.

The most general charges of any E_6 -motivated Z' model is generated by the linear combination of three independent sets of charges associated with the $U(1)_\kappa$ symmetries, where $\kappa = a, b, c$. In appendix Appendix C, we showed that for unification models the values of α and β corresponds to the vertical line which passes through Z_ψ and Z_χ . At low energies the parameter space of these models keeps close to this line, as can be seen in figure (6).

Without the unification hypothesis it is not possible to determine the preferred region in the parameter space. There are several models based on E_6 subgroups, and in some of them unification is not necessary to get a predictable model. In most of the well-known cases, the subgroup rank is less than the E_6 rank and at least one of the vector currents does not contribute to the electric charge. In order to ignore this current we set $\theta = 0$ in Eq. (12), in such a way that for a fixed value of the couplings the Z' charges reduce to a single point in the Sanson-Flamsteed projection. Since the values of the couplings is arbitrary, by varying them we generate the parameter space for these models.

For these models the hypercharge is the combination of the charges of two $U(1)$'s. If we put $k_c = 0$ and $\sin \theta = 0$, the charges in Eq. (12) reduce to

$$g_{Z'} \epsilon_{L,R}^{Z'} = g_Y \left(k_a \frac{\epsilon_{L,R}^b}{\hat{\beta}} - \hat{\beta} k_b \epsilon_{L,R}^a \right). \quad (28)$$

Owing to the fact that Q_c does not contribute to the electric charge, in these models is possible to have a low-energy theory without the corresponding Z'' associated with $U(1)_c$. In section 4 we denoted them as LEE6Ms. In E_6 there are three chains of subgroups where one of the Q_k corresponds to the SM hypercharge, in these cases, the SM is the LEE6M and, in principle, it does not require from other vector bosons to be a consistent theory. In Eq. (28) the U_a and U_b charges appear in a symmetric way, except by a global sign which, in general, can not be determined from the symmetry group.

In panel (6) the bottom-right figure shows the parameter space of some models based on E_6 subgroups. The horizontal dotted magenta line corresponds to the parameter space of the well-known LR models, which are LEE6Ms in the chains of subgroups $A2_R$, $B2_R$ and the $C3_R$. As expected, in this line appears the charges of the Z_{B-L} (U_{31R}) and Z_R (U_R). This line also represents the set of possible Z' models for flipped $SU(5)$ which are a linear combination of the $U_{\chi_{RA}}$ and U_{32A} . The

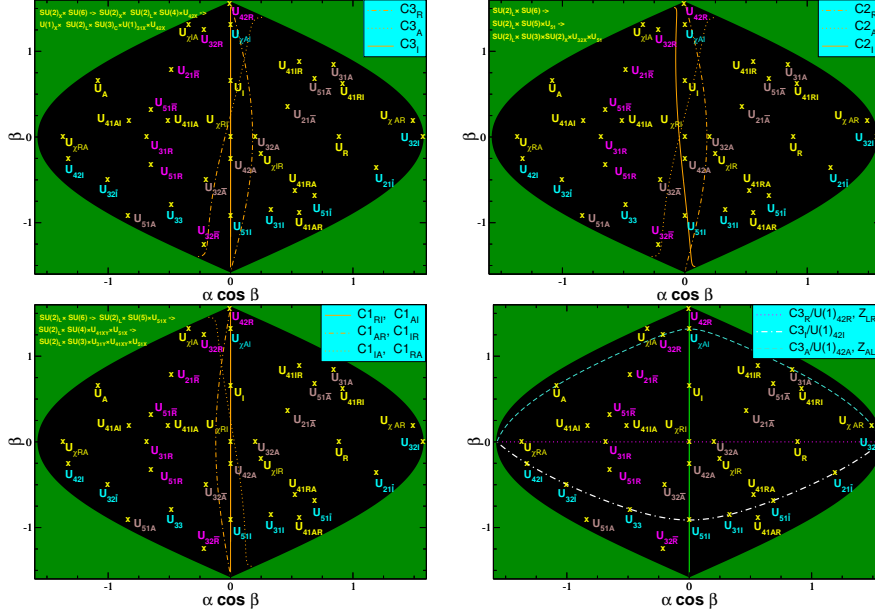


Fig. 6. Sanson-Flamsteed projection of the α - β parameter space in E_6 . The vertical line $\cos \beta = 0$ represent the models with charges orthogonal to the SM hypercharge, thus, deviations of this line show that at low energies there is a mixing between the Z' and the field associated with the SM hypercharge. To obtain the values of α and β in the top figures and in the bottom-left one we used the RGE² in order to get the g_a , g_b and g_c coupling strengths at the EW scale (from their initial values at the grand unification scale), then, we solved Eq. (C.1) varying θ between $-\pi$ and π . For the bottom-right figure, we put aside the unification hypothesis and, by ignoring the mixing with the fields associated with the charges that do not contribute to the electric charge, we explored the possible values for the coupling strengths; see section 5 for additional details.

dashed cyan line contains the Z' parameter space of the alternative left-right model Z_{ALR} . These models are the linear combination of U_{31A} and U_A (the downphobic model Z_d). This line also corresponds to the possible Z' of the LEE6M of the chain of subgroups $A1_{AR}$ which has not been reported in the literature, as far as we know. The dot-dashed gray line is the set of the possible Z' models of the LEE6M associated with the chain of subgroups $C4_I$ which contains the universal 331 model.^{13,40,46} We obtain these models from the linear combination of the $U(1)_{33}$ and the $U_{21\bar{I}}$, which have the quantum numbers of λ_{8L} and $U(1)'$ in the 331 models, respectively. This line is also generated from the third alternative left right model¹³ and results from the linear combination of U_{31I} (the leptophobic model Z_ℓ) and U_{42I} . This line also corresponds to the possible Z' for the LEE6M of $C2_I$, which, to the best of our knowledge, has not been reported in the literature. This set of points contains the Z_η (U_{51I}) model.

6. LHC constraints

Finally, we also report the most recent constraints from colliders and low-energy experiments on the neutral current parameters for some Z' -motivated E_6 models and the sequential standard model (SSM). For the time being, the strongest constraints come from the proton-proton collisions data collected by the ATLAS experiment at the LHC with an integrated luminosities of 36.1 fb^{-1} and 13.3 fb^{-1} at a center of mass energy of 13 TeV.^{52,53} In particular, we used the upper limits at 95% C.L. on the total cross-section of the Z' decaying into dileptons (*i.e.*, e^+e^- and $\mu^+\mu^-$). Figure (7) shows the contours of the lower limits on the $M_{Z'}$ at 95% C.L. We obtain these limits from the intersection of $\sigma^{\text{NLO}}(pp \rightarrow Z' \rightarrow l^-l^+)$ with the ATLAS 95% C.L. upper limits on the cross-section (for additional details see reference²¹). As a cross-check we calculated these limits for some models as shown in table 2 for various E_6 -motivated Z' models and the SSM model. In order to compare, we also show in this figure the constraints for all the models reported by ATLAS. For the 36.1 fb^{-1} data we multiply the theoretical cross-section by a global K factor to reproduce the ATLAS constraints for the Z_χ model. This procedure was not necessary for the 13.3 fb^{-1} dataset.

Table 2. 95% C.L. lower mass limits (in TeV) for E_6 -motivated Z' models and the sequential standard model Z_{SSM} . These constraints come from the 36.1 fb^{-1} and 13.3 fb^{-1} datasets for proton-proton collision at a center of mass energy of $\sqrt{s} = 13 \text{ TeV}$.^{52,53}

Z' model	luminosity	Z_χ	Z_ψ	Z_η	Z_{LR}	Z_R	Z_N	Z_S	Z_I	Z_{B-L}	Z_d	Z_{331G}	Z_{SSM}
$M_{Z'}(^{\dagger}\text{fitted})$	(36.1 fb^{-1})	4.1 [†]	3.81	3.91	4.28	4.41	3.84	4.02	3.94	4.44	4.66	4.608	4.58
ATLAS	(36.1 fb^{-1})	4.1	3.8	3.9	—	—	3.8	4.0	4.0	—	—	—	4.5
$M_{Z'}$	(13.3 fb^{-1})	3.62	3.35	3.43	3.77	3.92	3.38	3.54	3.47	3.95	4.15	4.10	4.05
ATLAS	(13.3 fb^{-1})	3.66	3.36	3.43	—	—	3.41	3.62	3.55	—	—	—	4.05

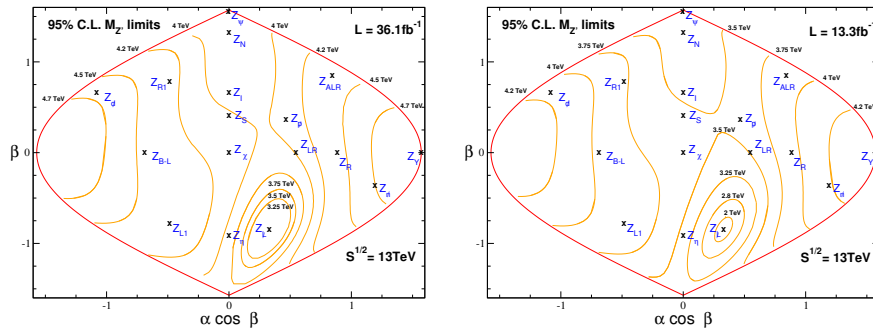


Fig. 7. α - β Sanson-Flamsteed projection of the Z' parameter space in E_6 . The contours show the 95% C.L. lower limits on the Z' mass (in TeV).

7. Conclusions

In the present work we have reported the most general expression for the chiral charges of a neutral gauge boson Z' coming from an E_6 unification model, in terms of the EW parameters and the charges of the $U(1)$ factors in the chain of subgroups.

We also showed for any breaking pattern that, the charges of SM hypercharge are orthogonal to the corresponding charges of the Z' gauge boson *i.e.*, $\sum_{f \in 27} Y(f)Q_{Z'}(f) = 0$ (see section 3), if the values of the g_κ coupling strengths associated with the $U(1)_\kappa$ factors of the chains of breakings are equal to each other. Due to the RGE the couplings are no longer identical at low energies, therefore there must be a mixing between the field associated with Y and the Z' . This mixing can modify several observables as it has been shown in reference.^{20,31,33}

Pure neutral gauge bosons coming from E_6 are Z_ψ and Z_χ as introduced in section 4.1 but the physical neutral states Z' and Z'' are a mixing of those states according to Eqs. (26) and (27), which define the α and β angles in our analysis. By using the RGE² and assuming E_6 unification, we showed that for most of the chains of breaking in E_6 it is possible to solve the equations for the mass scales in a consistent way (one important exception are the chains of subgroups that contain the Georgi-Glashow $SU(5)$ model and their alternative versions). This procedure allowed us to calculate the low-energy coupling strengths for several chains of subgroups and the Z' parameter space in the Sanson-Flamsteed projection. It is worth noting that in E_6 unification at low energies the parameter space of these models keeps close to the mentioned vertical line as can be seen in figure (6). To the best of our knowledge, several of the analyzed chains of subgroups presented here are new in the literature.

The most general charges of any E_6 -motivated Z' model is generated by the linear combination of three independent set of charges associated with the different $U(1)$ symmetries. By putting aside the unification hypothesis it is not possible to determine the preferred region in the parameter space; however, by ignoring the mixing with the associated charges that do not contribute to the electric charge, the corresponding parameter space reduces to a single line in the α - β Sanson-Flamsteed projection as shown for some models in the bottom right figure in (6).

By using the most recent upper limits on the cross-section for extra gauge vector bosons Z' decaying into dileptons from ATLAS data at 13 TeV with accumulated luminosities of 36.1fb^{-152} and 13.3fb^{-153} for the Drell-Yang processes $pp \rightarrow Z(\gamma) \rightarrow l^+l^-$, we set 95% C.L. lower limits on the Z' mass for the typical E_6 benchmark models. We also reported the contours in the 95% C.L. Z' mass limits for the entire Z' parameter space in E_6 . Our results are in agreement with the lower mass limits reported by ATLAS for the E_6 -motivated Z' models and the sequential standard model Z_{SSM} .

Finally it is important to stress that the recent LHCb anomalies could also be explained by E_6 subgroups.⁵⁴⁻⁵⁹ A natural continuation of our work would be to find which of these models are able to explain the anomalies. That is an interesting

16 *Richard H. Benavides, Luis Muñoz, William A. Ponce, Oscar Rodríguez, Eduardo Rojas*

question since the E_6 models, in general, have been considered as phenomenologically safe.

Acknowledgments

R. H. B. and L. M. thank the “Centro de Investigaciones ITM”. We thank Financial support from “Patrimonio Autónomo Fondo Nacional de Financiamiento para la Ciencia, la Tecnología y la Innovación, Francisco José de Caldas”, and “Sostenibilidad-UDEA”.

Appendix A. Rotation matrix

Let us now consider an explicit representation for the orthogonal matrix \mathcal{O} in terms of three angles ω , ϕ and θ , which are allowed to take values in the $[-\pi, \pi)$ interval. For convenience we choose

$$\mathcal{O} = \begin{pmatrix} 1 & 0 & 0 & 0 \\ 0 & \cos \omega & -\sin \omega & 0 \\ 0 & \sin \omega & \cos \omega & 0 \\ 0 & 0 & 0 & 1 \end{pmatrix} \begin{pmatrix} 1 & 0 & 0 & 0 \\ 0 & \cos \phi & 0 & -\sin \phi \\ 0 & 0 & 1 & 0 \\ 0 & \sin \phi & 0 & \cos \phi \end{pmatrix} \begin{pmatrix} 1 & 0 & 0 & 0 \\ 0 & 1 & 0 & 0 \\ 0 & 0 & \cos \theta & -\sin \theta \\ 0 & 0 & \sin \theta & \cos \theta \end{pmatrix}.$$

Relations in Eq.(10) imply then that

$$\cos \phi \cos \omega = \frac{k_a g_Y}{g_a}, \quad \cos \phi \sin \omega = \frac{k_b g_Y}{g_b}, \quad \sin \phi = \frac{k_c g_Y}{g_c}, \quad (\text{A.1})$$

which allows us to write the ϕ and ω angles in terms of the g_a and g_b coupling constants and of the k_a , k_b and k_c coefficients. The θ angle, however, cannot be fixed and must be considered to be another free-parameter. It is easy to show that

$$\cos \phi = \hat{\alpha}_c \frac{g_Y}{g_c}, \quad (\text{A.2})$$

$$\cos \omega = \frac{k_a g_c}{\hat{\alpha}_c g_a}, \quad (\text{A.3})$$

$$\sin \omega = \frac{k_b g_c}{\hat{\alpha}_c g_b}, \quad (\text{A.4})$$

where

$$\hat{\alpha}_c = g_c \sqrt{\frac{k_a^2}{g_a^2} + \frac{k_b^2}{g_b^2}} = \sqrt{\frac{g_c^2}{g^2} \cot^2 \theta_W - k_c^2}. \quad (\text{A.5})$$

Appendix B. Z' charges

From the Lagrangian

$$\begin{aligned} -\mathcal{L}_{NC} &= g J_{3L}^\mu A_{3L\mu} + g_a J_{a\mu} A_a^\mu + g_b J_{b\mu} A_b^\mu + g_c J_{c\mu} A_c^\mu \\ &= g_\kappa J_{\kappa\mu} A_\kappa^\mu = g_{\kappa''} J_{\kappa''\mu} \mathcal{O}_{\kappa''\kappa'}^T \mathcal{O}_{\kappa'\kappa}^T A_\kappa^\mu \\ &\equiv g_{\kappa'} J_{\kappa'\mu} Z_{\kappa'}^\mu, \end{aligned} \quad (\text{B.1})$$

where κ runs over $3L, a, b, c$ and k' and k'' runs over $3L, Y, Z', Z''$, from this equation we obtain

$$J_{\kappa'\mu} = J_{\kappa\mu} \mathcal{O}_{\kappa\kappa'} = \mathcal{O}_{\kappa'\kappa}^T J_{\kappa\mu} . \quad (\text{B.2})$$

From this equation the current associated with the Z' is given by^c

$$g_{Z'} J_{Z'} = g_Y \left(-\frac{k_a J_a^\mu + k_b J_b^\mu}{\hat{\alpha}_c} k_c + \hat{\alpha}_c J_c^\mu \right) \sin \theta + \frac{g_c}{\hat{\alpha}_c} \left(\frac{k_a J_b^\mu}{\hat{\beta}} - \hat{\beta} k_b J_a^\mu \right) \cos \theta , \quad (\text{B.3})$$

$$g_{Z''} J_{Z''} = g_Y \left(-\frac{k_a J_a^\mu + k_b J_b^\mu}{\hat{\alpha}_c} k_c + \hat{\alpha}_c J_c^\mu \right) \cos \theta - \frac{g_c}{\hat{\alpha}_c} \left(\frac{k_a J_b^\mu}{\hat{\beta}} - \hat{\beta} k_b J_a^\mu \right) \sin \theta , \quad (\text{B.4})$$

where $\hat{\beta} = \frac{g_a}{g_b}$. For the LEE6Ms ($c = 0$ and $\sin \theta = 0$) we obtain

$$g_{Z'} J_{g_{Z'}}^\mu = g_Y \left(k_a \frac{J_b^\mu}{\hat{\beta}} - \hat{\beta} k_b J_a^\mu \right) = g_Y \left(k_b \frac{J_b^\mu}{\hat{\alpha}_a} k_a - \hat{\alpha}_a J_a^\mu \right) \text{sign}(k_b) , \quad (\text{B.5})$$

$$= g_Y \left(\hat{\alpha}_b J_b^\mu - k_a \frac{J_a^\mu}{\hat{\alpha}_b} k_b \right) \text{sign}(k_a) , \quad (\text{B.6})$$

where

$$\hat{\alpha}_{a,b} = \sqrt{\frac{g_{a,b}^2}{g^2} \cot^2 \theta_W - k_{a,b}^2} . \quad (\text{B.7})$$

Appendix C. Sanson-Flamsteed Projection

As we mentioned in section 4 in general any Z' in E_6 can be written as a linear combination of three linear independent models. One usual basis is given by

$$\begin{aligned} g_{Z'} \epsilon_{L,R}^{Z'} &= g_{Z'} \left(\cos \alpha \cos \beta \epsilon_{L,R}^{Z_\chi} + \sin \alpha \cos \beta Y_{L,R} + \sin \beta \epsilon_{L,R}^{Z_\psi} \right) \eta , \\ &= A_{L,R} \sin \theta + B_{L,R} \cos \theta , \quad \text{with } \eta = \pm 1 , \end{aligned} \quad (\text{C.1})$$

where the $\epsilon_{L,R}^{Z_\chi}$ and $\epsilon_{L,R}^{Z_\psi}$ are the chiral charges of the Z_χ and Z_ψ models, respectively. In this equation $g_{Z'}$ is given by the Eq. 16. In the last line we equate the chiral charges for the Z' associated to a given chain of subgroups Eq. (12) to the general expression of the E_6 motivated Z' charges in the α - β parameter space Eq. 27. We can obtain the partial unification mass scales for every breaking pattern according to the reference^{2d}. By evolving g_a , g_b and g_c down to low energies for every θ there is a pair (α, β) according with the equation (C.1). θ parametrizes the mixing between the Z' and Z'' the charges (C.1) and the corresponding parameter space to low energies is shown in figure (6). It is important to notice that at low energies the charges keep close to the vertical line which corresponds to the unification parameter space.

^cWe have omitted a global sign which cannot be determined from the symmetry group.

^dFor some breakings there is some ambiguity, in these cases, we chose the lowest mass scale at its minimum value

Appendix D. tables

Table 3. E_6 normalized chiral charges of ordinary fermions and right-handed neutrinos. Here $l_L = (\nu_L, e_L)^T$ and $q_L = (u_L, d_L)^T$ denote the left-handed lepton and quark doublets.

Model	$\epsilon_L(l)$	$\epsilon_R(\nu)$	$\epsilon_R(e)$	$\epsilon_L(q)$	$\epsilon_R(u)$	$\epsilon(d)$
U_Y	$-\frac{1}{2}\sqrt{\frac{3}{5}}$	0	$-\sqrt{\frac{3}{5}}$	$\frac{1}{2\sqrt{15}}$	$\frac{2}{\sqrt{15}}$	$-\frac{1}{\sqrt{15}}$
U_R	0	$\frac{1}{2}$	$-\frac{1}{2}$	0	$\frac{1}{2}$	$-\frac{1}{2}$
U_I	$\frac{1}{2}$	$\frac{1}{2}$	0	0	0	$-\frac{1}{2}$
U_A	$\frac{1}{2}$	0	$\frac{1}{2}$	0	$-\frac{1}{2}$	0
U_{33}	$\frac{1}{2\sqrt{3}}$	$\frac{1}{\sqrt{3}}$	$\frac{1}{\sqrt{3}}$	$-\frac{1}{2\sqrt{3}}$	0	0
$U_{21\bar{R}}$	$\frac{1}{\sqrt{3}}$	$\frac{1}{2\sqrt{3}}$	$\frac{1}{2\sqrt{3}}$	0	$-\frac{1}{2\sqrt{3}}$	$-\frac{1}{2\sqrt{3}}$
$U_{21\bar{I}}$	$-\frac{1}{2\sqrt{3}}$	$\frac{1}{2\sqrt{3}}$	$-\frac{1}{\sqrt{3}}$	0	$\frac{1}{\sqrt{3}}$	$-\frac{1}{2\sqrt{3}}$
$U_{21\bar{A}}$	$\frac{1}{2\sqrt{3}}$	$\frac{1}{\sqrt{3}}$	$-\frac{1}{2\sqrt{3}}$	0	$\frac{1}{2\sqrt{3}}$	$-\frac{1}{\sqrt{3}}$
U_{31R}	$\frac{1}{2}\sqrt{\frac{3}{2}}$	$\frac{1}{2}\sqrt{\frac{3}{2}}$	$\frac{1}{2}\sqrt{\frac{3}{2}}$	$-\frac{1}{2\sqrt{6}}$	$-\frac{1}{2\sqrt{6}}$	$-\frac{1}{2\sqrt{6}}$
U_{31I}	0	$\frac{1}{2}\sqrt{\frac{3}{2}}$	0	$-\frac{1}{2\sqrt{6}}$	$\frac{1}{\sqrt{6}}$	$-\frac{1}{2\sqrt{6}}$
U_{31A}	0	0	$-\frac{1}{2}\sqrt{\frac{3}{2}}$	$\frac{1}{2\sqrt{6}}$	$\frac{1}{2\sqrt{6}}$	$-\frac{1}{\sqrt{6}}$
U_{42R}	$\frac{1}{2\sqrt{6}}$	$-\frac{1}{2\sqrt{6}}$	$-\frac{1}{2\sqrt{6}}$	$\frac{1}{2\sqrt{6}}$	$-\frac{1}{2\sqrt{6}}$	$-\frac{1}{2\sqrt{6}}$
U_{42I}	$\frac{1}{\sqrt{6}}$	$\frac{1}{2\sqrt{6}}$	$\sqrt{\frac{2}{3}}$	$-\frac{1}{2\sqrt{6}}$	$-\frac{1}{\sqrt{6}}$	$\frac{1}{2\sqrt{6}}$
U_{42A}	$\frac{1}{\sqrt{6}}$	$\sqrt{\frac{2}{3}}$	$\frac{1}{2\sqrt{6}}$	$-\frac{1}{2\sqrt{6}}$	$\frac{1}{2\sqrt{6}}$	$-\frac{1}{\sqrt{6}}$
U_{32R}	$\frac{1}{2}\sqrt{\frac{3}{5}}$	0	0	$\frac{1}{2\sqrt{15}}$	$-\frac{1}{\sqrt{15}}$	$-\frac{1}{\sqrt{15}}$
U_{32I}	$-\frac{1}{2}\sqrt{\frac{3}{5}}$	0	$-\sqrt{\frac{3}{5}}$	$\frac{1}{2\sqrt{15}}$	$\frac{2}{\sqrt{15}}$	$-\frac{1}{\sqrt{15}}$
U_{32A}	$\frac{1}{2}\sqrt{\frac{3}{5}}$	$\sqrt{\frac{3}{5}}$	0	$-\frac{1}{2\sqrt{15}}$	$\frac{1}{\sqrt{15}}$	$-\frac{2}{\sqrt{15}}$
$U_{32\bar{R}}$	0	$\frac{1}{2}\sqrt{\frac{3}{5}}$	$\frac{1}{2}\sqrt{\frac{3}{5}}$	$-\frac{1}{\sqrt{15}}$	$\frac{1}{2\sqrt{15}}$	$\frac{1}{2\sqrt{15}}$
$U_{32\bar{I}}$	$\frac{1}{2}\sqrt{\frac{3}{5}}$	$\frac{1}{2}\sqrt{\frac{3}{5}}$	$\sqrt{\frac{3}{5}}$	$-\frac{1}{\sqrt{15}}$	$-\frac{1}{\sqrt{15}}$	$\frac{1}{2\sqrt{15}}$
$U_{32\bar{A}}$	$\frac{1}{2}\sqrt{\frac{3}{5}}$	$\sqrt{\frac{3}{5}}$	$\frac{1}{2}\sqrt{\frac{3}{5}}$	$-\frac{1}{\sqrt{15}}$	$\frac{1}{2\sqrt{15}}$	$-\frac{1}{\sqrt{15}}$
U_{51R}	$\frac{2}{\sqrt{15}}$	$\frac{1}{2}\sqrt{\frac{5}{3}}$	$\frac{1}{2}\sqrt{\frac{5}{3}}$	$-\frac{1}{\sqrt{15}}$	$-\frac{1}{2\sqrt{15}}$	$-\frac{1}{2\sqrt{15}}$
U_{51I}	$\frac{1}{2\sqrt{15}}$	$\frac{1}{2}\sqrt{\frac{5}{3}}$	$\frac{1}{\sqrt{15}}$	$-\frac{1}{\sqrt{15}}$	$\frac{1}{\sqrt{15}}$	$-\frac{1}{2\sqrt{15}}$
U_{51A}	$\frac{1}{2\sqrt{15}}$	$\frac{1}{\sqrt{15}}$	$\frac{1}{2}\sqrt{\frac{5}{3}}$	$-\frac{1}{\sqrt{15}}$	$-\frac{1}{2\sqrt{15}}$	$\frac{1}{\sqrt{15}}$
$U_{51\bar{R}}$	$\frac{1}{2}\sqrt{\frac{5}{3}}$	$\frac{2}{\sqrt{15}}$	$\frac{2}{\sqrt{15}}$	$-\frac{1}{2\sqrt{15}}$	$-\frac{1}{\sqrt{15}}$	$-\frac{1}{\sqrt{15}}$
$U_{51\bar{I}}$	$-\frac{1}{2\sqrt{15}}$	$\frac{2}{\sqrt{15}}$	$-\frac{1}{\sqrt{15}}$	$-\frac{1}{2\sqrt{15}}$	$\frac{2}{\sqrt{15}}$	$-\frac{1}{\sqrt{15}}$
$U_{51\bar{A}}$	$\frac{1}{2\sqrt{15}}$	$\frac{1}{\sqrt{15}}$	$-\frac{2}{\sqrt{15}}$	$\frac{1}{2\sqrt{15}}$	$\frac{1}{\sqrt{15}}$	$-\frac{2}{\sqrt{15}}$
U_{41IA}	$\sqrt{\frac{2}{5}}$	$\sqrt{\frac{2}{5}}$	$\frac{3}{2\sqrt{10}}$	$-\frac{1}{2\sqrt{10}}$	$-\frac{1}{2\sqrt{10}}$	$-\frac{1}{\sqrt{10}}$
U_{41AR}	$-\frac{1}{2\sqrt{10}}$	$\frac{3}{2\sqrt{10}}$	$-\frac{1}{2\sqrt{10}}$	$-\frac{1}{2\sqrt{10}}$	$\frac{3}{2\sqrt{10}}$	$-\frac{1}{2\sqrt{10}}$
U_{41RI}	0	$\frac{1}{2\sqrt{10}}$	$-\sqrt{\frac{2}{5}}$	$\frac{1}{2\sqrt{10}}$	$\frac{1}{\sqrt{10}}$	$-\frac{3}{2\sqrt{10}}$
U_{41AI}	$\sqrt{\frac{2}{5}}$	$\frac{3}{2\sqrt{10}}$	$\sqrt{\frac{2}{5}}$	$-\frac{1}{2\sqrt{10}}$	$-\frac{1}{\sqrt{10}}$	$-\frac{1}{2\sqrt{10}}$
U_{41RA}	0	$\sqrt{\frac{2}{5}}$	$-\frac{1}{2\sqrt{10}}$	$-\frac{1}{2\sqrt{10}}$	$\frac{3}{2\sqrt{10}}$	$-\frac{1}{\sqrt{10}}$
U_{41IR}	$\frac{1}{2\sqrt{10}}$	$\frac{1}{2\sqrt{10}}$	$-\frac{3}{2\sqrt{10}}$	$\frac{1}{2\sqrt{10}}$	$\frac{1}{2\sqrt{10}}$	$-\frac{3}{2\sqrt{10}}$
$U_{\chi RI}$	$\frac{3}{2\sqrt{10}}$	$\frac{1}{2}\sqrt{\frac{5}{2}}$	$\frac{1}{2\sqrt{10}}$	$-\frac{1}{2\sqrt{10}}$	$\frac{1}{2\sqrt{10}}$	$-\frac{3}{2\sqrt{10}}$
$U_{\chi AR}$	$-\frac{1}{\sqrt{10}}$	0	$-\frac{1}{2}\sqrt{\frac{5}{2}}$	$\frac{1}{2\sqrt{10}}$	$\frac{3}{2\sqrt{10}}$	$-\frac{1}{\sqrt{10}}$
$U_{\chi IA}$	$\frac{1}{\sqrt{10}}$	$-\frac{1}{2\sqrt{10}}$	0	$\frac{1}{2\sqrt{10}}$	$-\frac{1}{\sqrt{10}}$	$-\frac{1}{2\sqrt{10}}$
$U_{\chi IR}$	$\frac{1}{\sqrt{10}}$	$\frac{1}{2}\sqrt{\frac{5}{2}}$	0	$-\frac{1}{2\sqrt{10}}$	$\frac{1}{\sqrt{10}}$	$-\frac{3}{2\sqrt{10}}$
$U_{\chi RA}$	$\frac{3}{2\sqrt{10}}$	$\frac{1}{2\sqrt{10}}$	$\frac{1}{2}\sqrt{\frac{5}{2}}$	$-\frac{1}{2\sqrt{10}}$	$-\frac{3}{2\sqrt{10}}$	$\frac{1}{2\sqrt{10}}$
$U_{\chi AI}$	$\frac{1}{\sqrt{10}}$	0	$-\frac{1}{2\sqrt{10}}$	$\frac{1}{2\sqrt{10}}$	$-\frac{1}{2\sqrt{10}}$	$-\frac{1}{\sqrt{10}}$

Table 4. Models arising from the $E_6 \rightarrow SO(10) \otimes U(1)_{42X} \rightarrow SU(3)_C \otimes SU(2)_L \otimes G \rightarrow G_{SM}$ chains of subgroups, where $G_{SM} \equiv SU(3)_C \otimes SU(2)_L \otimes U(1)_Y$.

Model	G factor				
$A1_{XY}$	$U(1)_{32Y} \otimes U(1)_{\chi XY} \otimes U(1)_{42X}$	k_a	k_b	k_c	
$A1_{IR}$	$U(1)_{32R} \otimes U(1)_{\chi IR} \otimes U(1)_{42I}$	$-\frac{1}{\sqrt{15}}$	$\frac{1}{\sqrt{10}}$	$-\sqrt{\frac{3}{2}}$	1, 24, 36 12 1
$A1_{AR}$	$U(1)_{32R} \otimes U(1)_{\chi AR} \otimes U(1)_{42A}$	$-\frac{1}{\sqrt{15}}$	$2\sqrt{\frac{2}{5}}$	0	
$A1_{RI}$	$U(1)_{32I} \otimes U(1)_{\chi RI} \otimes U(1)_{42R}$	$\sqrt{\frac{5}{3}}$	0	0	
$A1_{AI}$	$U(1)_{32I} \otimes U(1)_{\chi AI} \otimes U(1)_{42A}$	$\sqrt{\frac{5}{3}}$	0	0	
$A1_{RA}$	$U(1)_{32A} \otimes U(1)_{\chi RA} \otimes U(1)_{42R}$	$\frac{1}{\sqrt{15}}$	$-2\sqrt{\frac{2}{5}}$	0	
$A1_{IA}$	$U(1)_{32A} \otimes U(1)_{\chi IA} \otimes U(1)_{42I}$	$\frac{1}{\sqrt{15}}$	$-\frac{1}{\sqrt{10}}$	$-\sqrt{\frac{3}{2}}$	
$A2_X$	$U(1)_X \otimes U(1)_{31X} \otimes U(1)_{42X}$	k_a	k_b	k_c	
$A2_R$	$U(1)_R \otimes U(1)_{31R} \otimes U(1)_{42R}$	1	$-\sqrt{\frac{2}{3}}$	0	41, 47
$A2_I$	$U(1)_I \otimes U(1)_{31I} \otimes U(1)_{42I}$	0	$\frac{1}{\sqrt{6}}$	$-\sqrt{\frac{3}{2}}$	13
$A2_A$	$U(1)_A \otimes U(1)_{31A} \otimes U(1)_{42A}$	-1	$\sqrt{\frac{2}{3}}$	0	4
$A3_X$	$U(1)_{31X} \otimes U(1)_{42X}$	k_a	k_b		
$A3_R$	$U(1)_{31R} \otimes U(1)_{42R}$	--	--		
$A3_I$	$U(1)_{31I} \otimes U(1)_{42I}$	$\frac{1}{\sqrt{6}}$	$-\sqrt{3/2}$		
$A3_A$	$U(1)_{31A} \otimes U(1)_{42A}$	--	--		

Table 5. Models arising from the $E_6 \rightarrow SU(2)_X \otimes SU(6) \rightarrow SU(3)_C \otimes SU(2)_L \otimes G \rightarrow G_{SM}$ chains of subgroups, where $G_{SM} \equiv SU(3)_C \otimes SU(2)_L \otimes U(1)_Y$.

Model	G factor				
$B1_X$	$U(1)_{32X} \otimes U(1)_{51X} \otimes U(1)_X$	k_a	k_b	k_c	
$B1_R$	$U(1)_{32R} \otimes U(1)_{51R} \otimes U(1)_R$	$-\frac{1}{\sqrt{15}}$	$-\sqrt{\frac{3}{5}}$	1	3
$B1_I$	$U(1)_{32I} \otimes U(1)_{51I} \otimes U(1)_I$	$\sqrt{\frac{5}{3}}$	0	0	
$B1_A$	$U(1)_{32A} \otimes U(1)_{51A} \otimes U(1)_A$	$\frac{1}{\sqrt{15}}$	$-\sqrt{\frac{3}{5}}$	-1	
$B2_X$	$U(1)_{31X} \otimes U(1)_{42X} \otimes U(1)_X$	same as	$A2_X$		
$B3_X$	$U(1)_{33} \otimes U(1)_{21\bar{X}} \otimes U(1)_X$	same as	D_X		

20 *Richard H. Benavides, Luis Muñoz, William A. Ponce, Oscar Rodríguez, Eduardo Rojas*

Table 6. Models arising from the $E_6 \rightarrow SU(2)_L \otimes SU(6) \rightarrow SU(3)_C \otimes SU(2)_L \otimes G \rightarrow G_{SM}$ chains of subgroups, where $G_{SM} \equiv SU(3)_C \otimes SU(2)_L \otimes U(1)_Y$.

Model	G factor			
$C1_{XY}$	$U(1)_{31Y} \otimes U(1)_{41XY} \otimes U(1)_{51\bar{X}}$	k_a	k_b	k_c
$C1_{IR}$	$U(1)_{31R} \otimes U(1)_{41IR} \otimes U(1)_{51\bar{I}}$	$-\sqrt{\frac{2}{3}}$	$\sqrt{\frac{2}{5}}$	$\sqrt{\frac{3}{5}}$
$C1_{AR}$	$U(1)_{31R} \otimes U(1)_{41AR} \otimes U(1)_{51\bar{A}}$	$-\sqrt{\frac{2}{3}}$	$\sqrt{\frac{2}{5}}$	$\sqrt{\frac{3}{5}}$
$C1_{RI}$	$U(1)_{31I} \otimes U(1)_{41RI} \otimes U(1)_{51\bar{R}}$	$\frac{1}{\sqrt{6}}$	$\frac{3}{\sqrt{10}}$	$-\sqrt{\frac{3}{5}}$
$C1_{AI}$	$U(1)_{31I} \otimes U(1)_{41AI} \otimes U(1)_{51\bar{A}}$	$\frac{1}{\sqrt{6}}$	$-\frac{3}{\sqrt{10}}$	$\sqrt{\frac{3}{5}}$
$C1_{RA}$	$U(1)_{31A} \otimes U(1)_{41RA} \otimes U(1)_{51\bar{R}}$	$\sqrt{\frac{2}{3}}$	$\sqrt{\frac{2}{5}}$	$-\sqrt{\frac{3}{5}}$
$C1_{IA}$	$U(1)_{31A} \otimes U(1)_{41IA} \otimes U(1)_{51\bar{I}}$	$\sqrt{\frac{2}{3}}$	$-\sqrt{\frac{2}{5}}$	$\sqrt{\frac{3}{5}}$
$C2_X$	$U(1)_X \otimes U(1)_{32\bar{X}} \otimes U(1)_{51\bar{X}}$	k_a	k_b	k_c
$C2_R$	$U(1)_R \otimes U(1)_{32\bar{R}} \otimes U(1)_{51\bar{R}}$	1	$-\frac{1}{\sqrt{15}}$	$-\sqrt{\frac{3}{5}}$
$C2_I$	$U(1)_I \otimes U(1)_{32\bar{I}} \otimes U(1)_{51\bar{I}}$	0	$-\frac{4}{\sqrt{15}}$	$\sqrt{\frac{3}{5}}$
$C2_A$	$U(1)_A \otimes U(1)_{32\bar{A}} \otimes U(1)_{51\bar{A}}$	-1	$-\frac{1}{\sqrt{15}}$	$\sqrt{\frac{3}{5}}$
$C3_X$	$U(1)_X \otimes U(1)_{31X} \otimes U(1)_{42X}$	same as $A2_X$		
$C4_X$	$U(1)_X \otimes U(1)_{21\bar{X}} \otimes U(1)_{33}$	same as D_X		

Table 7. Models arising from the $E_6 \rightarrow SU(3) \otimes SU(3) \otimes SU(3) \rightarrow SU(3)_C \otimes SU(2)_L \otimes G \rightarrow G_{SM}$ chains of subgroups, where $G_{SM} \equiv SU(3)_C \otimes SU(2)_L \otimes U(1)_Y$.

Model	G factor				
D_X	$U(1)_X \otimes U(1)_{21\bar{X}} \otimes U(1)_{33}$	k_a	k_b	k_c	
D_R	$U(1)_R \otimes U(1)_{21\bar{R}} \otimes U(1)_{33}$	1	$-\frac{1}{\sqrt{3}}$	$-\frac{1}{\sqrt{3}}$	13, 23, 48–50
D_I	$U(1)_I \otimes U(1)_{21\bar{I}} \otimes U(1)_{33}$	0	$\frac{2}{\sqrt{3}}$	$-\frac{1}{\sqrt{3}}$	
D_A	$U(1)_A \otimes U(1)_{21\bar{A}} \otimes U(1)_{33}$	-1	$\frac{1}{\sqrt{3}}$	$-\frac{1}{\sqrt{3}}$	

References

1. S. M. Barr, *Phys. Lett.* **112B**, 219 (1982), doi:10.1016/0370-2693(82)90966-2.
2. R. W. Robinett and J. L. Rosner, *Phys. Rev.* **D26**, 2396 (1982), doi:10.1103/PhysRevD.26.2396.
3. E. Witten, *Nucl. Phys.* **B258**, 75 (1985), doi:10.1016/0550-3213(85)90603-0.

4. E. Ma, *Phys. Rev.* **D36**, 274 (1987), doi:10.1103/PhysRevD.36.274.
5. E. Ma, *Phys. Lett.* **B380**, 286 (1996), [arXiv:hep-ph/9507348 \[hep-ph\]](#), doi:10.1016/0370-2693(96)00524-2.
6. R. Martinez, W. A. Ponce and L. A. Sanchez, *Phys. Rev.* **D65**, 055013 (2002), [arXiv:hep-ph/0110246 \[hep-ph\]](#), doi:10.1103/PhysRevD.65.055013.
7. E. Rojas and J. Erler, *JHEP* **10**, 063 (2015), [arXiv:1505.03208 \[hep-ph\]](#), doi:10.1007/JHEP10(2015)063.
8. S. F. Mantilla, R. Martinez, F. Ochoa and C. F. Sierra, *Nucl. Phys.* **B911**, 338 (2016), [arXiv:1602.05216 \[hep-ph\]](#), doi:10.1016/j.nuclphysb.2016.08.014.
9. C.-S. Huang, W.-J. Li and X.-H. Wu (2017), [arXiv:1705.01411 \[hep-ph\]](#).
10. A. E. Cárcamo Hernández, S. Kovalenko, J. W. F. Valle and C. A. Vaquera-Araujo, *JHEP* **07**, 118 (2017), [arXiv:1705.06320 \[hep-ph\]](#), doi:10.1007/JHEP07(2017)118.
11. J. P. Derendinger, J. E. Kim and D. V. Nanopoulos, *Phys. Lett.* **139B**, 170 (1984), doi:10.1016/0370-2693(84)91238-3.
12. S. F. King, S. Moretti and R. Nevzorov, *Phys. Rev.* **D73**, 035009 (2006), [arXiv:hep-ph/0510419 \[hep-ph\]](#), doi:10.1103/PhysRevD.73.035009.
13. O. Rodríguez, R. H. Benavides, W. A. Ponce and E. Rojas, *Phys. Rev.* **D95**, 014009 (2017), [arXiv:1605.00575 \[hep-ph\]](#), doi:10.1103/PhysRevD.95.014009.
14. S. Dimopoulos and L. J. Hall, *Nucl. Phys.* **B255**, 633 (1985), doi:10.1016/0550-3213(85)90157-9.
15. J. Rizos and K. Tamvakis, *Phys. Lett.* **B414**, 277 (1997), [arXiv:hep-ph/9702295 \[hep-ph\]](#), doi:10.1016/S0370-2693(97)01181-7.
16. Q. Shafi and Z. Tavartkiladze, *Nucl. Phys.* **B552**, 67 (1999), [arXiv:hep-ph/9807502 \[hep-ph\]](#), doi:10.1016/S0550-3213(99)00178-9.
17. A. E. Faraggi, M. Paraskevas, J. Rizos and K. Tamvakis, *Phys. Rev.* **D90**, 015036 (2014), [arXiv:1405.2274 \[hep-ph\]](#), doi:10.1103/PhysRevD.90.015036.
18. P. V. Dong, D. T. Huong, F. S. Queiroz, J. W. F. Valle and C. A. Vaquera-Araujo (2017), [arXiv:1710.06951 \[hep-ph\]](#).
19. R. Benavides, L. A. Muñoz, W. A. Ponce, O. Rodríguez and E. Rojas, *Phys. Rev.* **D95**, 115018 (2017), [arXiv:1612.07660 \[hep-ph\]](#), doi:10.1103/PhysRevD.95.115018.
20. P. Langacker, *Rev. Mod. Phys.* **81**, 1199 (2009), [arXiv:0801.1345 \[hep-ph\]](#), doi:10.1103/RevModPhys.81.1199.
21. C. Salazar, R. H. Benavides, W. A. Ponce and E. Rojas, *JHEP* **07**, 096 (2015), [arXiv:1503.03519 \[hep-ph\]](#), doi:10.1007/JHEP07(2015)096.
22. F. Gursey, P. Ramond and P. Sikivie, *Phys. Lett.* **60B**, 177 (1976), doi:10.1016/0370-2693(76)90417-2.
23. Y. Achiman and B. Stech, *Phys. Lett.* **77B**, 389 (1978), doi:10.1016/0370-2693(78)90584-1.
24. D. London and J. L. Rosner, *Phys. Rev.* **D34**, 1530 (1986), doi:10.1103/PhysRevD.34.1530.
25. J. E. Camargo-Molina, A. P. Morais, A. Ordell, R. Pasechnik and J. Wessén (2017), [arXiv:1711.05199 \[hep-ph\]](#).
26. J. Erler, *Nucl. Phys.* **B586**, 73 (2000), [arXiv:hep-ph/0006051 \[hep-ph\]](#), doi:10.1016/S0550-3213(00)00427-2.
27. M. Carena, A. Daleo, B. A. Dobrescu and T. M. P. Tait, *Phys. Rev.* **D70**, 093009 (2004), [arXiv:hep-ph/0408098 \[hep-ph\]](#), doi:10.1103/PhysRevD.70.093009.
28. J. Erler, P. Langacker, S. Munir and E. Rojas, *JHEP* **11**, 076 (2011), [arXiv:1103.2659 \[hep-ph\]](#), doi:10.1007/JHEP11(2011)076.
29. R. Slansky, *Phys. Rept.* **79**, 1 (1981), doi:10.1016/0370-1573(81)90092-2.
30. J. Erler, P. Langacker, S. Munir and E. Rojas, *JHEP* **08**, 017 (2009), [arXiv:0906.2435](#)

22 *Richard H. Benavides, Luis Muñoz, William A. Ponce, Oscar Rodríguez, Eduardo Rojas*

- [hep-ph], doi:10.1088/1126-6708/2009/08/017.
31. B. Holdom, *Phys. Lett.* **166B**, 196 (1986), doi:10.1016/0370-2693(86)91377-8.
 32. K. S. Babu, C. F. Kolda and J. March-Russell, *Phys. Rev.* **D54**, 4635 (1996), [arXiv:hep-ph/9603212](#) [hep-ph], doi:10.1103/PhysRevD.54.4635.
 33. K. S. Babu, C. F. Kolda and J. March-Russell, *Phys. Rev.* **D57**, 6788 (1998), [arXiv:hep-ph/9710441](#) [hep-ph], doi:10.1103/PhysRevD.57.6788.
 34. F. del Aguila, G. D. Coughlan and M. Quiros, *Nucl. Phys.* **B307**, 633 (1988), doi:10.1016/0550-3213(88)90266-0, [Erratum: Nucl. Phys.B312,751(1989)].
 35. L. Baulieu and R. Coquereaux, *Annals Phys.* **140**, 163 (1982), doi:10.1016/0003-4916(82)90339-6.
 36. H. Georgi and S. L. Glashow, *Phys. Rev. Lett.* **32**, 438 (1974), doi:10.1103/PhysRevLett.32.438.
 37. J. Erler, P. Langacker, S. Munir and E. Rojas, *AIP Conf. Proc.* **1200**, 790 (2010), [arXiv:0910.0269](#) [hep-ph], doi:10.1063/1.3327731.
 38. J. Erler, P. Langacker, S. Munir and E. rojas, 'Z' searches: From tevatron to lhc, in *22nd Rencontres de Blois on Particle Physics and Cosmology Blois, Loire Valley, France, July 15-20, 2010*, .
 39. J. Erler, P. Langacker, S. Munir and E. Rojas, 'Z' Bosons from E(6): Collider and Electroweak Constraints, in *19th International Workshop on Deep-Inelastic Scattering and Related Subjects (DIS 2011) Newport News, Virginia, April 11-15, 2011*, (2011). [arXiv:1108.0685](#) [hep-ph].
 40. L. A. Sanchez, W. A. Ponce and R. Martinez, *Phys. Rev.* **D64**, 075013 (2001), [arXiv:hep-ph/0103244](#) [hep-ph], doi:10.1103/PhysRevD.64.075013.
 41. J. C. Pati and A. Salam, *Phys. Rev.* **D10**, 275 (1974), doi:10.1103/PhysRevD.10.275, 10.1103/PhysRevD.11.703.2, [Erratum: Phys. Rev.D11,703(1975)].
 42. S. L. Glashow, *Nucl. Phys.* **22**, 579 (1961), doi:10.1016/0029-5582(61)90469-2.
 43. S. Weinberg, *Phys. Rev. Lett.* **19**, 1264 (1967), doi:10.1103/PhysRevLett.19.1264.
 44. J. Erler, P. Langacker and T.-j. Li, *Phys. Rev.* **D66**, 015002 (2002), [arXiv:hep-ph/0205001](#) [hep-ph], doi:10.1103/PhysRevD.66.015002.
 45. J. Kang, P. Langacker, T.-j. Li and T. Liu, *Phys. Rev. Lett.* **94**, 061801 (2005), [arXiv:hep-ph/0402086](#) [hep-ph], doi:10.1103/PhysRevLett.94.061801.
 46. M. Singer, J. W. F. Valle and J. Schechter, *Phys. Rev.* **D22**, 738 (1980), doi:10.1103/PhysRevD.22.738.
 47. R. N. Mohapatra and J. C. Pati, *Phys. Rev.* **D11**, 566 (1975), doi:10.1103/PhysRevD.11.566.
 48. Y. Achiman, *Phys. Lett.* **70B**, 187 (1977), doi:10.1016/0370-2693(77)90517-2.
 49. S. L. Glashow, Trinification of All Elementary Particle Forces, in *Fifth Workshop on Grand Unification Providence, Rhode Island, April 12-14, 1984*, (1984), p. 0088.
 50. K. S. Babu, X.-G. He and S. Pakvasa, *Phys. Rev.* **D33**, 763 (1986), doi:10.1103/PhysRevD.33.763.
 51. Y. Bai and B. A. Dobrescu (2017), [arXiv:1710.01456](#) [hep-ph].
 52. ATLAS Collaboration (M. Aaboud *et al.*), *JHEP* **10**, 182 (2017), [arXiv:1707.02424](#) [hep-ex], doi:10.1007/JHEP10(2017)182.
 53. ATLAS Collaboration (T. A. collaboration) (2016).
 54. C. Hati, G. Kumar and N. Mahajan, *JHEP* **01**, 117 (2016), [arXiv:1511.03290](#) [hep-ph], doi:10.1007/JHEP01(2016)117.
 55. A. Joglekar and J. L. Rosner, *Phys. Rev.* **D96**, 015026 (2017), [arXiv:1607.06900](#) [hep-ph], doi:10.1103/PhysRevD.96.015026.
 56. D. Das, C. Hati, G. Kumar and N. Mahajan, *Phys. Rev.* **D94**, 055034 (2016), [arXiv:1605.06313](#) [hep-ph], doi:10.1103/PhysRevD.94.055034.

- 57. I. Doršner, S. Fajfer, D. A. Faroughy and N. Košnik (2017), [arXiv:1706.07779](#) [[hep-ph](#)], doi:10.1007/JHEP10(2017)188, [JHEP10,188(2017)].
- 58. M. Blanke and A. Crivellin (2018), [arXiv:1801.07256](#) [[hep-ph](#)].
- 59. O. Popov and G. A. White, *Nucl. Phys.* **B923**, 324 (2017), [arXiv:1611.04566](#) [[hep-ph](#)], doi:10.1016/j.nuclphysb.2017.08.007.